IOSR Journal of Mechanical and Civil Engineering (IOSR-JMCE)
e-ISSN: 2278-1684,p-ISSN: 2320-334X, Volume 14, Issue 4 Ver. VII (Jul. - Aug. 2017), PP 17-21
www.iosrjournals.org

Analysis of Te inclusions in CdMnTe Being Developed for the Detection of X-Rays and Gamma-Rays

Mebougna L. Drabo[1,2], Aaron L. Adams[1,2], Alexander A. Egarievwe[1,2], Kristina C. Fonz[3], Stephen U. Egarievwe[2,4], Utpal N. Roy[4], Ralph B. James[5]

[1](*Department of Mechanical & Civil Engineering, and Construction Management, Alabama A&M University, Normal, AL 35762, USA)*
[2](*Nuclear Engineering and Radiological Science Center, Alabama A&M University, Normal, AL 35762, USA)*
[3](*Department of Psychology, University of Alabama at Birmingham, Birmingham, AL, USA)*
[4](*Department of Nonproliferation and National Security, Brookhaven National Laboratory, Upton, NY, USA)*
[5](*Science and Technology, Savannah River National Laboratory, Aiken, SC, USA)*
*Corresponding Author: * Mebougna L. Drabo*

Abstract: *Large tellurium inclusions in the matrix of as-grown cadmium manganese telluride (CdMnTe) crystals limit their ability to detect X-rays and gamma-rays at high resolutions. CdMnTe has potential applications in high-resolution nuclear and radiological detection at room-temperature. Defects associated with tellurium inclusions trap charges generated when CdMnTe detectors are irradiated with X-rays and gamma rays. This degrades the charge transport properties of the detectors and reduces lifetime of the charge carriers, which results in poor performance by the detector. Post-growth thermal annealing is often used to remove tellurium inclusions from the CdMnTe matrix. In this paper, we present analysis of the distribution of tellurium inclusions CdMnTe wafers that were annealed at 720 ℃ and in cadmium vapor. The tellurium inclusions were imaged using infrared transmission microscopy. The two-dimensional analysis of the observed changes to the sizes of the tellurium inclusions showed that some were completing eliminated, while others were reduced in their dimensions. The average size reduction for Te inclusions of diameters below 9 μm is about 40% while that for inclusion above 10 μm is about 5%. The diameters of the Te inclusion that were completing eliminated are below 5 μm. are reductions in the dimensions of the medium-size Te inclusions. Several Te inclusion with diameters less than 6 μm dissipated into smaller inclusions. The diameters of the resulting smaller Te inclusions are less than 1 μm.*

Keywords: *CdMnTe, gamma-rays, infrared microscopy, tellurium inclusions, thermal annealing, X-rays.*

Date of Submission: 16 -08-2017 Date of acceptance: 28-08-2017

I. Introduction

Cadmium manganese telluride (CdMnTe) is one of the tertiary compounds of cadmium telluride (CdTe) semiconductor material with potential applications in nuclear and radiological detection at room temperature without cryogenic cooling. Room-temperature semiconductor detectors have the advantages of low operation cost and production of portable and hand-held devices for the detection of X-rays and gamma-rays. [1]-[3]. There have been recent interests in cadmium manganese telluride (CdMnTe) for room-temperature nuclear and radiological detection applications [4]-[8]. This is due to the segregation coefficient of Mn in cadmium telluride (CdTe) matrix that is about 1.0 that could result in the growth of detector-grade CdMnTe crystals with uniform Mn content and high homogeneity [7], [8].

The presence of Te inclusions and related defects in detector wafers is a major problem with CdMnTe crystals, especially those grown by the Bridgman technique. This problem is also found CdZnTe [13]. The tellurium inclusions and associated defects trap charges generated when CdMnTe detectors are irradiated with X-rays and gamma rays. This degrades the charge transport properties of the detectors and reduces lifetime of the charge carriers, which results in poor performance by the detector. Post-growth thermal annealing is often used to remove tellurium inclusions from the CdMnTe matrix. The wafers can be annealed at a *constant temperature* in a Cd vapor, or annealed under a *temperature gradient* to induce the migration of Te inclusions to the high-temperature side of the sample. The annealing temperature is often around or above the melting point of Te. Cadmium from Cd-rich atmosphere diffuses into the CdMnTe matrix constant temperature annealing, and combines with excess Te to form crystalline material. As for temperature-gradient annealing, the migration of Te particles to one side leaves regions with fewer and smaller Te inclusions, which can be harvested for detector fabrication [9]. In our previous report, we presented how annealing in Cd vapor affects Te inclusions and the electrical resistivity of CdMnTe crystals [9]. For CdMnTe wafer annealed at 720 °C, we reported reductions in

size of Te inclusions, with some Te inclusions eliminated while others broke up to smaller sizes [9]. Also, the resistivity of the CdMnTe wafer was reduced by 71 %, from 2.44 x 10^5 Ω-cm to 7.17 x 10^4 Ω-cm after annealing in Cd vapor. In this paper, we present a two-dimensional (2D) analysis of the distribution of tellurium inclusions the CdMnTe wafers before and after annealing at 720 °C and in cadmium vapor.

II. Experiment

The 4.5 mm x 4.0 mm x 1.5 mm wafer used in this experiment was cut from a CdMnTe grown by the Bridgman technique [4]. The detailed of the annealing experiment is described by Adams et al. [9]. The wafer was first polished with 800-grit and 1200-grit silicon carbide abrasive papers, followed by successive polishing on multi-tex pads with alumina powder of sizes 3 microns, 1 micron, and 0.1 micron. In the Infrared (IR) transmission microscopy used to image the Te inclusions, an AmScope Camera MD900E was adjusted to record the IR images. The Te inclusions are opaque to IR light while the CdMnTe matrix is transparent. The electrical resistivity of the sample was measured before and after annealing of the sample. This was accomplished by depositing Au electrical contacts by electroless technique using a gold chloride ($AuCl_3$) solution, and measuring the bulk leakage current for every applied voltage using a Keithley Picoammeter/Voltage Source [9]. The electrical contacts were removed from the samples through successive polishing on multi-tex pads with alumina powder of sizes 3 microns, 1 micron, and 0.1 micron.

The thermal annealing process involves sealing the CdMnTe wafer and shots of Cd in a quartz ampoule under a vacuum of 10^{-5} mbar. The CdMnTe wafer was placed at one side of the ampoule and Cd was placed at the opposite side as shown in Fig. 1. It is advisable to have a constriction between them to prevent the sticking together of the Cd shots and the wafer during annealing. A three-zone furnace was used for annealing the wafer. The temperature profile of the furnace was obtained using a thermocouple, and the desired annealing temperature was obtained by adjusting the three heating elements of the furnace. The sample was annealed at 720 °C for 12 hours.

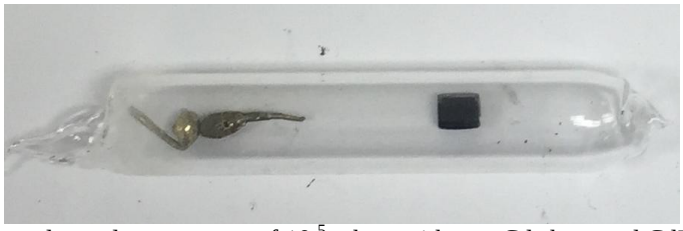

Fig. 1. Sealed quartz ampoule, under a vacuum of 10^{-5} mbar, with two Cd shots and CdMnTe wafer. The length of the ampoule is approximately 5 cm.

III. Results and Discussions

The infrared images of a 256 μm x 367 μm region of the CdMnTe wafer before and after annealing in Cd vapor are shown in Fig. 2 along with the diameters (in μm) of the Te inclusions. The diameters of the Te inclusions in Fig. 2 were measured using ImageJ software. Te inclusions less than 1 μm in diameter were observed in Fig 2b.

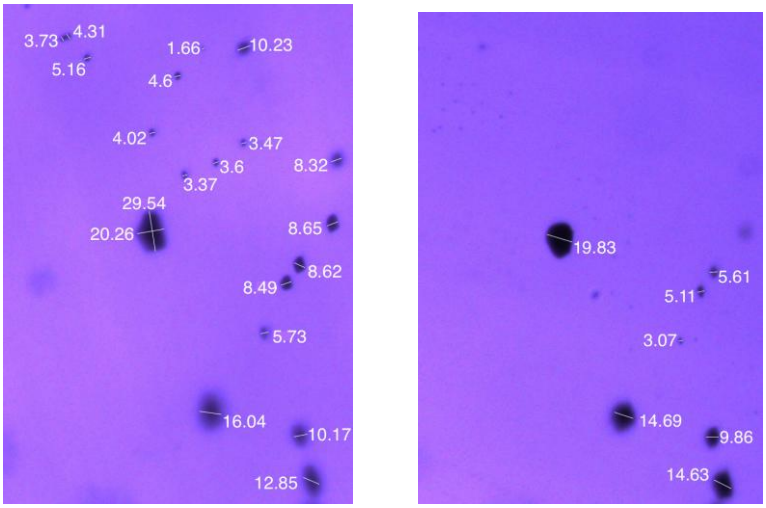

(a) Before annealing (256 μm x 367 μm) (b) After annealing (256 μm x 367 μm)

Fig. 2. Infrared images of the same region of the CdMnTe wafer before and after annealing in Cd vapor. The diameter of the Te inclusions are in μm.

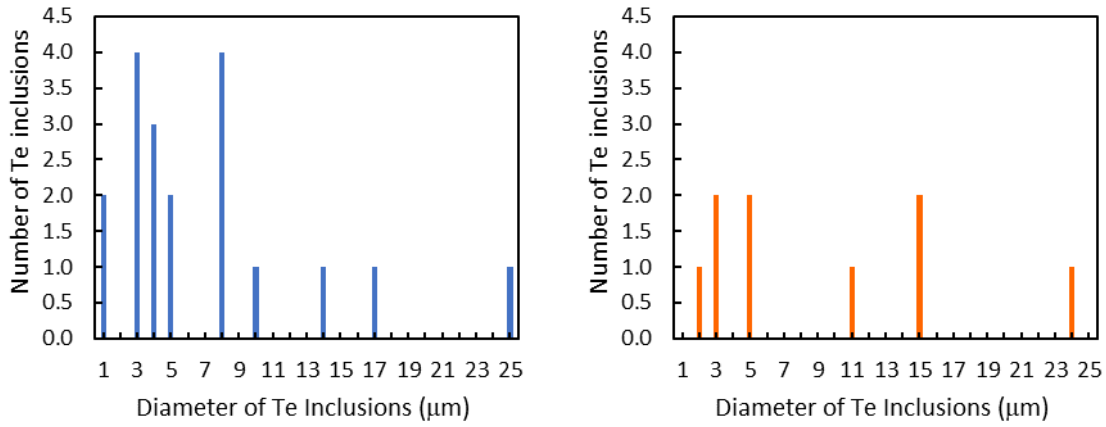

(a) Before annealing (b) After annealing

Fig. 3. Infrared images of the same region of the CdMnTe wafer before and after annealing in Cd vapor.

The number of different sizes of Te inclusions, before and after annealing, in the 256 μm x 367 μm region of the sample are shown in Fig. 3. This shows a reduction in the size of Te inclusions. Fig. 2 shows only one measurement across each Te inclusion. Since many of the Te inclusions are not perfectly spherical, the diameters were estimated from the average of several measurements across the center from two opposite ends. The reductions in the sizes of selected Te inclusions after annealing are shown in Table 1. These are typical representations of Te inclusions in the CdMnTe wafer before and after annealing. The Te inclusions in the upper third of Fig. 2 are not shown in Table 1 because they appear to have been eliminated (as in the upper right region) or separated into smaller inclusions with diameters less than 1 μm (as in the upper left region). The large Te inclusion in the bottom right corner of Fig. 2 appeared to have increased in size. This could be due to other smaller inclusions that fused with the large inclusion during the annealing process. From Table 1, one could see that the smaller Te inclusion have larger size reduction after annealing, compare to the large inclusions. The average size reduction for Te inclusions of diameters below 9 μm is about 40% while that for inclusion above 10 μm is about 5%.

Table 1: Reduction in the size of Te inclusions after annealing the sample in Cd vapor.

Diameter of Te Inclusion Before Annealing (μm)	Diameter of Te Inclusion After Annealing (μm)	Reduction in Size of Te Inclusion
5.7	3.1	46%
8.5	5.1	40%
8.7	5.6	36%
10.2	9.9	3%
16.1	14.9	7%
24.8	23.7	4%

The 3D visualization of the transparency of the Te inclusions are shown in Fig. 4 for the sample before annealing, and in Fig. 5 after annealing in Cd vapor. The 3D images were made using MATLAB and TECPLOT software packages. The X, Y and Z axes in Fig. 4 and Fig. 5 have arbitrary units. The value of the X side is 256 μm and that of the Y side is 367 μm. The values of the transparencies are relative (they are not the absolute values).

IV. Conclusions

This covered the analysis of the distribution of tellurium inclusions CdMnTe wafer annealed at 720 C and in cadmium vapor. The tellurium inclusions are opaque to infrared light while the CdZnTe matrix is transparent. Thus, we imaged the Te inclusions using infrared transmission microscopy. The two-dimensional analysis of the dimensions of the tellurium inclusions showed three categories of changes: 1) some Te inclusion were completing eliminated, 2) other Te inclusions were reduced in their dimensions, and some appear to dissipate into Te of smaller dimensions. The average size reduction for Te inclusions of diameters below 9 μm is about 40%. The average size reduction for inclusion above 10 μm is about 5%.

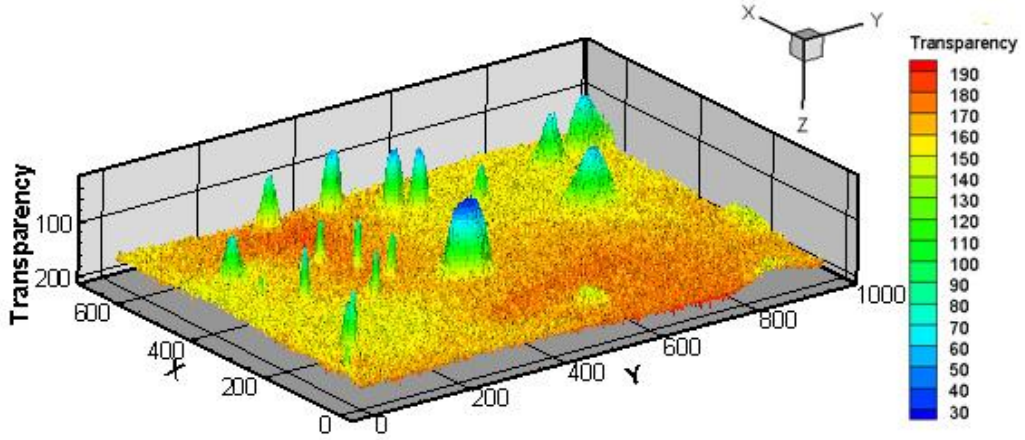

Fig. 4. Visualization in 3D of the Te inclusions in the sample before annealing. The X, Y and Z axes have arbitrary units. The values of the X and Y sides are 256 μm and 367 μm respectively. The values of the transparencies are relative (they are not the absolute values).

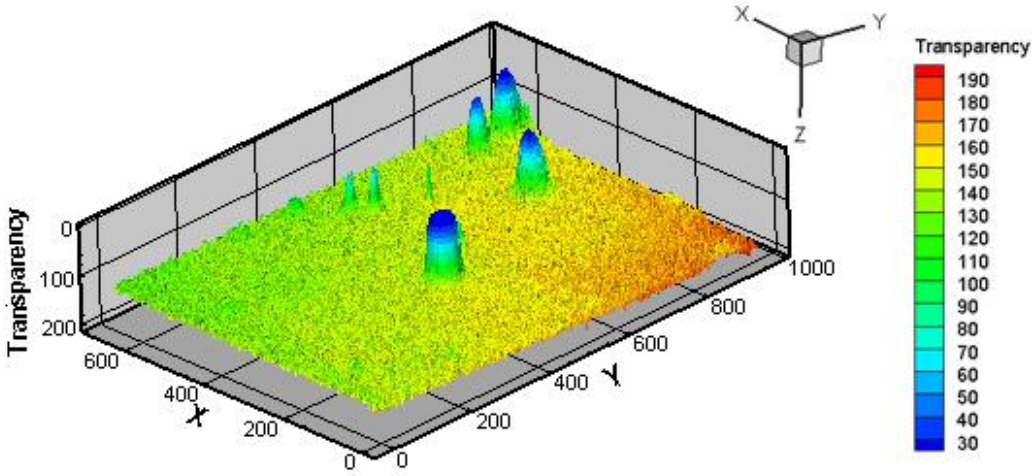

Fig. 5. Visualization in 3D of t the Te inclusions after annealing in Cd vapor. The X, Y and Z axes have arbitrary units. The values of the X and Y sides are 256 μm and 367 μm respectively. The values of the transparencies are relative (they are not the absolute values).

The diameters of the Te inclusion that were completing eliminated are below 5 μm. The Te inclusions that dissipated into smaller (< 1 μm in diameter) inclusions are less than 6 μm in diameter. The observed changes could be attributed to two major processes, 1) reaction between Te inclusions and Cd that diffused into the CdMnTe matrix, and 2) diffusion of Te within the matrix. [10]. The observed Te inclusion of sizes less than 1 μm that appeared in the CdMnTe matrix after annealing could be have come from dissipation of larger Te inclusions or diffusion from other regions of the wafer.

Acknowledgements

This work has been supported by the U.S. Department of Homeland Security, Domestic Nuclear Detection Office, under competitively awarded contract/IAA award number 2012-DN-077-ARI065-05, and the U.S. Nuclear Regulatory Commission through award numbers NRC-27-10-514 and NRC-HQ-84-16-G-0014.

References

[1] S. U. Egarievwe, W. Chan, K.-H. Kim, U. N. Roy, V. Sams, A. Hossain, A. Kassu, R. B. James. "Carbon Coating and Defects in CdZnTe and CdMnTe Nuclear Detectors," *IEEE Transactions on Nuclear Science, 63(1),* 2016, 236–245.

[2] N. Dedek, R. D. Speller, P. Spendley, and J. A. Horrocks, "Performance Evaluation of 98 CZT Sensors for Their Use in Gamma-Ray Imaging," *IEEE Transactions on Nuclear Science, 55(5),* 2008, 2689–2697.

[3] H. Chen, S. A. Awadalla, P. Marthandam, K. Iniewski, P. H. Lu, G. Bindley, "CZT device with improved sensitivity for medical imaging and homeland security applications," *Proc. SPIE 7449, Hard X-Ray, Gamma-Ray, and Neutron Detector Physics XI*, San Diego, CA, 2009, 744902.

[4] U. N. Roy, G. S. Camarda, Y. Cui, G. Gu, R. Gul, b, A. Hossain, G. Yang, S. U. Egarievwe, R. B. James. "Growth and characterization of CdMnTe by the vertical Bridgman technique," *Journal of Crystal Growth, 437,* 2016, 53–58.

[5] R. Rafiei, M. I. Reinhard, K. Kim, D. A. Prokopovich, D. Boardman, A. Sarbutt, G. C. Watt, A. E. Bolotnikov, L. J. Bignell, and R. B. James, "High-Purity CdMnTe Radiation Detectors: A High-Resolution Spectroscopic Evaluation," *IEEE Transactions on Nuclear Science, 60(2),* 2013, 1450–1456.

[6] Y. Du, W. Jie, X. Zheng, T. Wang, X. Bai, H. Yu, "Growth interface of In-doped CdMnTe from Te solution with vertical Bridgman method under ACRT technique", *Trans. Nonferrous Met. Soc. of China, 22*, 2012, s143−s147.

[7] A. Hossain, Y. Cui, A. E. Bolotnikov, G. S. Camarda, G. Yang, D. Kochanowska, M. Witkowska-Baran, A. Mycielski and R. B. James, "Vanadium-doped cadmium manganese telluride crystals as X- and gamma-ray detectors," *Journal of Electronic Materials, 38,* 2009, 1593–1599.

[8] Y. Du, W. Jie, T. Wang, Y. Xu, L. Yin, Pe. Yu, Ga. Zha, "Vertical Bridgman growth and characterization of CdMnTe crystals for gamma-ray radiation detector," *Journal of Crystal Growth, 318*, 2011, 1062–1066.

[9] A. L. Adams, E. O. Agbalagba, J. O. Jow, J. G. Mwathi, A. A. Egarievwe, W. Chan, M. C. Dowdell, U. N. Roy, S. U. Egarievwe. "Thermal Annealing of CdMnTe Material Being Developed for Nuclear Radiation Detection Applications." *IOSR Journal of Mechanical and Civil Engineering, 13(4),* ver IV 2016, 1 – 5.

[10] S. U. Egarievwe, G. Yang, A. A. Egarievwe, I. O. Okwechime, J. Gray, Z. M. Hales, A. Hossain, G. S. Camarda, A. E. Bolotnikov, and R. B. James, "Post-Growth Annealing of Bridgman-Grown CdZnTe and CdMnTe Crystals for Room-Temperature Nuclear Radiation Detectors." *Nuclear Instrumentation and Methods in Physics Research A*, 784, 2015, 51–55.

Mebougna L. Drabo. "Analysis of Te inclusions in CdMnTe Being Developed for the Detection of X-Rays and Gamma-Rays." IOSR Journal of Mechanical and Civil Engineering (IOSR-JMCE) , vol. 14, no. 4, 2017, pp. 17–21.